Current Issue

Volume 115, Number 3
March 2007

Recent In-Press

Childhood Leukemia in the Vicinity of the Gees...
Hoffmann W, et al.

Concentrations of Urinary Phthalate Metabolite...
Stahlhut RW, et al.

The Association between Blood Lead Levels and ...
Campbell JR, et al.

Di-(2-ethylhexyl) Phthalate Metabolites May Al...
Meeker JD, et al.

Silicatosis in a Carpet Installer. A Case Pres...
Szeinuk J, et al.

Household Air Pollution from Coal and Biomass ...
Zhang J, et al.

(More**)**

Recent Correspondence

Pfiesteria in Estuarine Waters: The Question o...
Shoemaker RC, et al.

(More**)**

ehp Science Education
Teachers: Download *EHP* Student Edition and Science Lessons for Free!

Get Instant Updates with *EHP* RSS Feeds

Environmental Health Perspectives Supplements Volume 106, Number S4, August 1998

- Related EHP Articles
- PubMed:Related Articles
- PubMed:Citation
- Cited in PMC
- Purchase This Issue

Experimental Investigations of the Entrapment and Persistence of Organic Liquid Contaminants in the Subsurface Environment

Linda M. Abriola and Scott A. Bradford

University of Michigan, Department of Civil and Environmental Engineering, Ann Arbor, Michigan

Abstract
Organic liquids are common polluters of the subsurface environment. Once released, these nonaqueous phase liquids (NAPLs) tend to become entrapped within soils and geologic formations where they may serve as long-term contaminant reservoirs. The interphase mass transfer from such entrapped residuals will ultimately control environmental exposure levels as well as the persistence and/or remedial recovery of these contaminants in the subsurface. This paper summarizes National Institute of Environmental Health Sciences-sponsored research designed to investigate and quantify NAPL entrapment and interphase mass transfer in natural porous media. Results of soil column and batch experiments are presented that highlight research findings over the past several years. These experiments explore dissolution and volatilization of hydrocarbons and chlorinated solvents in sandy porous media. Initial concentration levels and long-term recovery rates are shown to depend on fluid flow rate, soil structure, NAPL composition, and soil wetting characteristics. These observations are explained in the context of conceptual models that describe entrapped NAPL morphology and boundary layer transport. The implications of these laboratory findings on the subsurface persistence and recovery of entrapped NAPLs are discussed. -- **Environ Health Perspect** 106(Suppl 4):1083-1095 (1998).

Abstract

Organic liquids are common polluters of the subsurface environment. Once released, these nonaqueous phase liquids (NAPLs) tend to become entrapped within soils and geologic formations where they may serve as long-term contaminant reservoirs. The interphase mass transfer from such entrapped residuals will ultimately control environmental exposure levels as well as the persistence and/or remedial recovery of these contaminants in the subsurface. This paper summarizes National Institute of Environmental Health Sciences-sponsored research designed to investigate and quantify NAPL entrapment and interphase mass transfer in natural porous media. Results of soil column and batch experiments are presented that highlight research findings over the past several years. These experiments explore dissolution and volatilization of hydrocarbons and chlorinated solvents in sandy porous media. Initial concentration levels and long-term recovery rates are shown to depend on fluid flow rate, soil structure, NAPL composition, and soil wetting characteristics. These observations are explained in the context of conceptual models that describe entrapped NAPL morphology and boundary layer transport. The implications of these laboratory findings on the subsurface persistence and recovery of entrapped NAPLs are discussed. -- **Environ Health Perspect** 106(Suppl 4) :1083-1095 (1998) .

http://ehpnet1.niehs.nih.gov/docs/1998/Suppl-4/1083-1095abriola/abstract.html

Key words: nonaqueous phase liquids, entrapment, mass transfer, contamination, remediation, groundwater

This paper is based on a presentation at the Symposium on the Superfund Basic Research Program: A Decade of Improving Health through Multi-Disciplinary Research held 23-26 February 1997 in Chapel Hill, North Carolina. Manuscript received at *EHP* 11 December 1997; accepted 23 April 1998.

Funding for this research was provided by the National Institute of Environmental Health Sciences grant ES04911 under the Superfund Basic Research Program. Partial funding for some of the early dissolution studies was also provided by the U.S. Department of Energy, Office of Health and Environmental Research, Subsurface Science Program under grant F60289-ER60844.

Address correspondence to L.M. Abriola, University of Michigan, Department of Civil and Environmental Engineering, 181 EWRE, 1351 Beal Avenue, Ann Arbor, MI 48109-2125. Telephone: (313) 763-9664. Fax: (313) 763-2275. E-mail: abriola@engin.umich.edu

Abbreviations used: see "Appendix."

Introduction

Of the most frequently detected soil and groundwater pollutants at National Priorities listed hazardous waste sites, the large majority are known chemical constituents of organic liquid contaminants. (See compounds marked with an asterisk in Table 1.) Included among these organic liquids, commonly known as nonaqueous phase liquids (NAPLs), are petroleum fuels, chlorinated solvents, transmission oils, and coal tars. As Table 1 suggests, NAPLs are ubiquitous in the contaminated subsurface. A National Research Council review of 77 contaminated sites (*1*) revealed that more than two-thirds of these sites were contaminated by NAPLs.

Table 1. The twenty-five most frequently detected groundwater contaminants at hazardous waste sites.[a]

Rank	Compound	Common sources
1*	Trichloroethylene	Dry cleaning; metal degreasing
2*	Lead	Gasoline (prior to 1975); mining; construction material (piped); manufacturing
3*	Tetrachloroethylene	Dry cleaning; metal degreasing
4*	Benzene	Gasoline; manufacturing
5*	Toluene	Gasoline; manufacturing
6	Chromium	Metal plating
7*	Methylene chloride	Degreasing; solvents; paint removal
8	Zinc	Manufacturing; mining
9*	1,1,1-Trichloroethane	Metal and plastic cleaning
10	Arsenic	Mining; manufacturing
11*	Chloroform	Solvents
12*	1,1-Dichloroethene	Degreasing; solvents
13*	1,2-Dichloroethene, trans-	Transformation product of 1,1,1-trichloroethane
14	Cadmium	Mining; plating
15	Manganese	Manufacturing; mining; occurs in nature as oxide
16	Copper	Manufacturing; mining
17*	1,1-Dichloroethene	Manufacturing
18*	Vinyl chloride	Plastic and record manufacturing
19	Barium	Manufacturing; energy production
20*	1,2-Dichloroethane	Metal degreasing; paint removal
21*	Ethylbenzene	Styrene and asphalt manufacturing; gasoline
22	Nickel	Manufacturing; mining
23*	Di(2-ethylhexyl)phthalate	Plastics manufacturing
24*	Xylenes	Solvents; gasoline
25*	Phenol	Wood treating; medicines

This ranking was generated by the Agency for Toxic Substances and Disease Registry using groundwater data from the National Priorities List of sites to be cleaned up under the Comprehensive Environmental Response, Compensation, and Liability Act. The ranking is based on the number of sites at which the substance was detected in ground water. [a]Modified from the NRC (*1*). *Known constituent of organic liquid contaminants.

Organic liquids are commonly released through underground storage tank and piping leaks, surface spills, and improper disposal practices (*2*). Most of these organic liquids are only sparingly soluble (immiscible) in water and many components have low volatility. Thus, once introduced into the subsurface, they tend to persist in the environment as a distinct organic phase that can serve as a long-term source of air and water contamination. Indeed, it is now widely recognized that the presence of NAPLs is one of the most significant factors limiting the success of conventional "pump-and-treat" groundwater remediation technologies (*3*).

When an organic liquid penetrates the subsurface, it tends to migrate downwards under gravity until it encounters a soil region of low fluid conductivity or until it reaches the water-saturated soil zone. As it migrates downwards, capillary forces act to retain a portion of the organic liquid within the soil matrix. This retained portion is known as NAPL residual. Upon reaching the saturated soil zone or a lower conductivity layer, the NAPL may migrate laterally until a balance is achieved between pressure, gravity, and capillary forces. For NAPLs with densities significantly greater than water (DNAPLs), the saturated soil zone may not act as an impediment to vertical migration and the DNAPL will continue to move downwards under gravity forces, leaving entrapped organic residual in its wake. Downward migration will continue until complete retention or until the DNAPL encounters a low conductivity or impermeable zone, where it will spread laterally. Depending upon the soil texture, entrapped residual organic saturations may vary from approximately 4 to 10% of the pore space in the unsaturated soil zone (*4*) to as high as 20% of the pore space in the saturated zone (*5*,*6*).

Due to the low solubilities and often low volatilities of many NAPLs, the bulk of the contaminant mass in the subsurface tends to reside in the NAPL phase, persisting as a long-term contamination source. Thus, if one is interested in predicting contaminant concentrations that will be measured at receptor wells or within the atmosphere in the vicinity of a hazardous waste site, an understanding of NAPL interphase mass partitioning behavior is crucial. In addition to its influence on exposure levels, the extent and rates of interphase mass transfer will also control the persistence of organic contaminants in the subsurface environment and the bioavailability of such compounds for natural microbial transformations. An understanding of interphase mass transfer could also guide the development and design of innovative remediation or containment/barrier technologies, such as soil vapor extraction and bioventing (*7*), surfactant or solvent-enhanced aquifer remediation (*8*,*9*), or *in situ* soil property modification strategies (*10*,*11*).

The objective of this paper is to present an overview of fundamental laboratory research exploring NAPL interphase mass transfer conducted during the last few years under sponsorship of the National Institute of Environmental Health Sciences (NIEHS) Superfund Basic Research Program at the University of Michigan, Ann Arbor, Michigan (*4*,*6*,*12-16*). The overview is intended to provide the scientifically educated nonspecialist with a general understanding of the findings and implications of this research. The material presented herein is based upon an invited lecture presented at an interdisciplinary meeting of the NIEHS Superfund Basic Research Program investigators held in February 1997 in Chapel Hill, North Carolina. Due to the broadness of the topic and the scope of material covered, no attempt has been made to present an exhaustive review of the related scientific literature. However, results of NIEHS-sponsored studies are presented in the context of other investigations.

An overview is by nature selective. Thus, illustrative results and research highlights are offered to provide a coherent description of the thrust of the research. It must be noted at the outset that many individuals have contributed to the work presented herein. Their names are acknowledged below through references to published articles, abstracts, and reports. The interested reader is referred to these references for more detailed information.

Conceptual Model of Interphase Mass Transfer

Conceptual models of pore fluid distributions in a NAPL contaminated region of

the subsurface are presented in Figure 1. Figure 1A depicts a two-fluid-phase (water-organic) system that is representative of NAPL entrapment within the saturated soil zone. In sketching this figure, it has been assumed that water tends to preferentially wet the soil grains. This will be the case for common soil constituents such as quartz and carbonates (*17*). Under these conditions, water is called the wetting phase; in larger pores, it occupies the volume immediately adjacent to the soil grains and it tends to occupy the entire volume of the smaller pores. In contrast, the NAPL tends to form entrapped ganglia, which are discontinuous blobs of organic liquid within the center of the larger pores. Figure 1A suggests that ganglia may be quite complex in shape, occupying multiple pore bodies. These shapes are controlled by variations in pore structure and size, as well as by the initial organic release rate. Studies in etched glass micromodels that mimic the pore structure in natural media (*18*) and observations of ganglia cast within porous media (*5*,*6*,*12*) have confirmed this conceptual model.

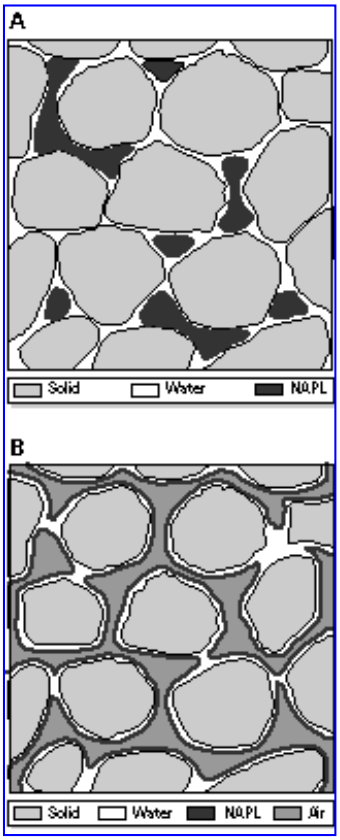

Figure 1. Hypothetical distribution of residual NAPL in the saturated (*A*) and unsaturated (*B*) zones when the porous medium is water-wet.

In a contaminated unsaturated soil zone, three fluid phases will be present: water, organic, and gas (air). Figure 1B depicts the configuration of these fluids within the pores of such a system. Here again, water preferentially wets the solid surface and tends to occupy the entire volume of the smallest pores. The center of the largest pores, however, is now occupied by the soil gas. The entrapped organic liquid tends to spread along the water-gas interfaces, forming continuous films, lenses, or wedges. This conceptual model is consistent with fluid distributions observed in etched glass micromodels (*18*,*19*) and in natural sands that were frozen and sectioned (*20*).

When a NAPL is entrapped within the saturated or unsaturated soil zones, the migration of contaminants that are constituents of this organic liquid is ultimately controlled by the exchange of mass between the organic and the soil water (dissolution) and/or gas (volatilization) phases. Figure 2 depicts the exchange of mass across the interface between a single component NAPL and the α (water or gas) phase. A boundary layer is assumed to occur at the interface separating the residual NAPL and the bulk flowing α phase. The thickness of this boundary layer will be a function of the viscosity and velocity of the α phase. Mass exchange across this boundary layer may occur in a series of steps (*21*). First, the organic partitions into the α phase at the interface according to equilibrium thermodynamics. This partitioning process may also be influenced by surface phenomena such as sorption or chemical reactions. Next, the organic diffuses through the boundary layer into the bulk α phase. This boundary layer diffusion is often considered to be the process that controls the rate of interphase mass transfer (*4*,*22*,*23*).

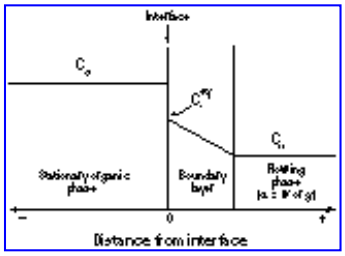

Figure 2. The spatial variation of the organic concentration at the interface separating the organic and α phases (α = *w* or *g* for water and gas, respectively) according to the linear driving force model.

A quasi-steady approximation may be developed from Fick's first law for diffusion through the boundary layer. It

is given by the following linear driving force expression:

$$J^{o\alpha} = k^{o\alpha}\left(C_\alpha^{eq} - C_\alpha\right) \qquad [1]$$

Here $J^{o\alpha}$ represents the flux of the organic (*o*) to the α phase (M L^{-2} t^{-1}). The concentration driving force is approximated by the difference between the equilibrium (C_α^{eq}) and the bulk phase (C_α) concentrations of the organic in the α phase; the value of C_α^{eq} is believed to approximate the concentration at the interface. The coefficient of proportionality in Equation 1 ($k^{o\alpha}$), is known as the mass transfer coefficient (L t^{-1}). According to Fick's first law, $k^{o\alpha}$ will be inversely related to the thickness of the boundary layer and directly proportional to the diffusivity of the organic in the bulk α phase. Consistent with experimental observations, however, the value of $k^{o\alpha}$ is typically modeled in particular applications as a nonlinear function of diffusivity, velocity, and viscosity (*23*).

To determine the total mass exchanged during some time interval using Equation 1, information must be available on the total interfacial area across which this mass transfer is occurring. The direct measurement or estimation of interfacial areas is a difficult task due to spatial and temporal changes in NAPL configuration. It is customary, then, to represent interfacial mass transfer in terms of a lumped mass transfer coefficient ($\hat{k}^{oa} = a^{o\alpha} k^{o\alpha}$) ($t^{-1}$) that is the product of the mass transfer coefficient and the specific interfacial area ($a^{o\alpha}$) (the interfacial area per unit volume of porous medium). Thus, the mass exchanged per unit time per unit volume between the organic and α phases becomes ($E^{o\alpha}$):

$$E^{o\alpha} = J^{o\alpha} a^{o\alpha} = \hat{k}^{oa}\left(C_\alpha^{eq} - C_\alpha\right) \qquad [2]$$

It should be noted that more complicated alternative mathematical expressions have been postulated in the literature to describe interphase mass transfer in porous media. Such models may incorporate more than one rate-limiting process, relax the quasi-steady assumption, or divide the domain into regions in which different mechanisms are controlling. Most of these models were developed to describe sorption phenomena [for review, see Weber et al. (*21*)]. Although some investigators have extended such models to the NAPL interphase mass transfer problem (*24-26*), few independent estimates for model parameters exist and these models have not been applied to scenarios that involve changing interfacial areas. The mass transfer experiments presented in this paper have been interpreted in the context of Equation 2. This choice is based upon the simplicity of this expression and its implicit incorporation of interfacial area.

Application of Equation 2 requires knowledge of the lumped mass transfer coefficient. Chemical and environmental engineers have developed dimensionless correlations representing the relationship between relevant system parameters and experimentally determined mass transfer coefficients for a variety of porous media systems (*6*,*27-35*). These correlations frequently incorporate the mass transfer coefficient in terms of a dimensionless Sherwood number. In the present work and many previous NAPL dissolution studies, a modified Sherwood number ($Sh^{o\alpha}$) is defined in terms of the lumped mass transfer coefficient as

$$Sh^{o\alpha} = \frac{\hat{k}^{oa}\left(d_{50}\right)^2}{D_\alpha} \qquad [3]$$

Here d_{50}, the mean grain size, is chosen as the length scale and D^α is the free liquid diffusivity of the organic component in the α phase. Other dimensionless variables that are commonly included in mass transfer correlations include the Reynolds number (*Re*)

$$Re = \frac{\rho_\alpha v_\alpha d_{50}}{\mu_\alpha} \quad [4]$$

and the Schmidt number (*Sc*):

$$Sc = \frac{\mu_\alpha}{D_\alpha \rho_\alpha} \quad [5]$$

where $\rho_\alpha, \mu_\alpha, v_\alpha$ are the density, viscosity, and average pore velocity of the α phase, respectively. It should be mentioned that individual correlations have been developed for particular systems under a limited range of conditions. Thus, caution should be exercised when applying such correlations to contaminated sites that are not representative of the experimental conditions for which these correlations were derived.

Dissolution and Volatilization of Pure Nonaqueous-Phase Liquids

Over the past several years, a systematic laboratory investigation has been undertaken to explore the dissolution and volatilization of entrapped NAPLs in soils. Here emphasis has been placed on the quantification of interphase mass transfer rates and the dependence of these rates on soil and fluid properties. Although a number of related laboratory-scale studies have appeared in the literature for selected experimental systems (*27*,*28*,*36-39*), the experimental investigations summarized herein are unique in the range of conditions explored. Initial experiments were conducted on pure (single component) organic liquids in homogeneous sandy media. Subsequent efforts have been directed towards exploring the influence of heterogeneities in soil and organic liquid composition on NAPL interphase mass transfer processes. These topics will be addressed later in the sections "Fractional Wettability Soils" and "NAPL Mixtures."

An illustrative schematic of the experimental setup for exploration of NAPL entrapment and mass transfer is presented in Figure 3. All experiments were conducted under one-dimensional flow conditions in custom-designed soil columns. These columns were approximately 5 cm in diameter and of varying lengths (3-10 cm), depending upon the experimental system. Fluid emplacement procedures were developed for two- and three-phase NAPL entrapment. These procedures were designed to ensure uniform and reproducible entrapment under conditions representative of environmental releases of contaminants to the saturated and unsaturated soil zones, respectively. Entrapped organic liquids included representative petroleum hydrocarbons and chlorinated solvents. Natural sandy media spanning a range of sand size fractions and gradation were employed in these investigations. The experimental protocols included uniform packing with a sandy porous medium, complete water saturation of the pores, and subsequent water displacement by NAPL injection (two-phase) or water drainage under suction (three-phase). Water drainage was then followed by water injection (two-phase) or NAPL injection and drainage (three-phase). The resultant NAPL residual volumetric fraction was determined gravimetrically. Following NAPL entrapment, columns were injected with water (two-phase) or purified nitrogen at high relative humidity (three-phase) under steady flow conditions. Concentrations of the organic contaminant in the column effluent were measured by high-pressure liquid chromatography (HPLC) or gas chromatography (GC). In all cases, linear calibration curves were established by comparison of retention time and detector response with known standards. Fluid flow rates were varied within ranges typical of natural and remediation flushing conditions. Volatilization measurements were conducted under controlled temperature conditions to minimize variations in equilibrium partial pressures and gas diffusivities over the course of an experiment. For a more detailed description of experimental protocols, the reader is referred to Powers et al. (*6*) and Wilkins et al. (*4*).

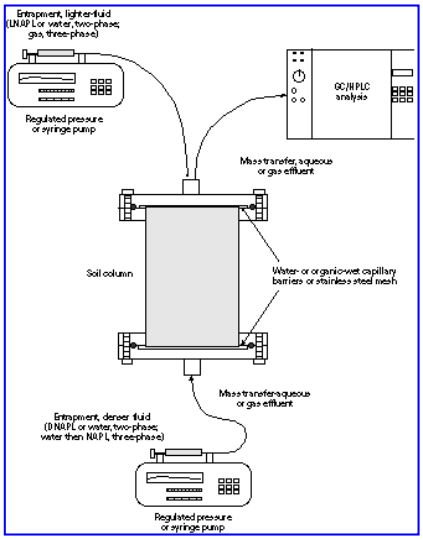

Figure 3. A general schematic of the soil column experimental setup used for NAPL entrapment and mass transfer studies. LNAPL, light nonaqueous phase liquid.

Representative measurements of initial NAPL dissolution in two sandy media are shown in Figure 4. Here column effluent concentrations have been normalized to the equilibrium solubility of the organic liquid (styrene) in water. Styrene is a model NAPL with properties representative of a petroleum hydrocarbon. It has a density less than that of water (0.907 g/cm^3) and an aqueous solubility of 230 mg/l at 25°C. The coarser and more uniform Ottawa sand was packed to a porosity of 0.318 and had an initial styrene saturation of 0.111, whereas the finer and more graded Wagner sand was packed to a porosity of 0.404 and had an initial styrene saturation equal to 0.139. Each data point in Figure 4 represents a measurement of concentration under quasi-steady (stabilized concentration) conditions at a particular water injection rate. For plotting purposes, injection rates have been divided by the cross-sectional area of the column to yield a superficial velocity. It should be noted that less than 10% of the initial entrapped NAPL mass was dissolved over the course of any particular experiment. Thus, it is reasonable to assume that the lumped mass transfer coefficient varies only in response to variations in the mass transfer coefficient for each sand, i.e., it is assumed that the interfacial area remains relatively constant over this time interval for a particular sand.

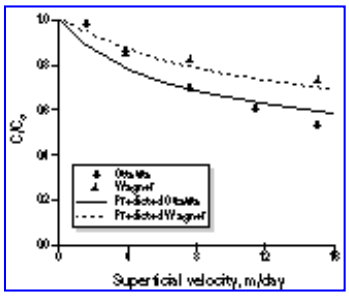

Figure 4. Plot of observed and predicted (Equation 6) normalized styrene effluent concentration as a function of the superficial velocity for Ottawa (d_{50}=0.071 cm, U=1.21) and Wagner (d_{50}=0.045 cm, U=1.45) sands (*6*); the Ottawa 20-30 sand was packed to a porosity of 0.318 and had an initial styrene saturation of 0.111; the Wagner #50 was packed to a porosity of 0.387 and had an initial saturation of 0.111.

Examination of Figure 4 reveals that dissolution was mass transfer rate limited in these experiments, that is, effluent concentrations differ from the equilibrium solubility of styrene. The figure also shows that deviations from equilibrium depend strongly on fluid velocity, increasing with increasing velocity. This effect is not unexpected as an increasing velocity reduces the contact time between the aqueous and NAPL phases in the column, and one would anticipate that the total mass transfer would decrease as a result. The data plotted in Figure 4 also suggest a marked dependence of dissolution mass transfer on soil physical characteristics. Here increasing grain size is linked to increasing deviations from equilibrium.

Based upon the data presented in Figure 4 and similar dissolution measurements in a variety of sandy media, Powers et al. (*6*,*12*) developed the following correlation expression for the lumped mass transfer coefficient:

$$Sh'^{ow} = 4.13 Re^{0.60} \delta^{0.67} U^{0.37} \qquad [6]$$

where $\delta = d_{50}/d_M$ and $U = d_{60}/d_{10}$ are the dimensionless mean grain size and the uniformity index, respectively; the parameter d_M=0.05 cm is defined as the mean grain size of a medium sand (*40*), and d_{60} and d_{10} are the soil grain sizes for which 60 and 10%, respectively, of the sand mass is finer. Here, a uniformity index of 1 indicates that the medium is composed of grains of uniform size and an increasing value of *U* indicates more variation in the grain size distribution.

The above correlation was developed using a multiple linear regression technique to determine the best fit correlation for the experimental data. The coefficient of multiple determination (R^2) and standard error estimate for Equation 6 were 0.94 and 0.062, respectively. This correlation was developed for a range of Reynolds numbers (0.015-0.20), mean grain sizes (0.045-0.12 cm), and uniformity indices (1.19-3.46). Equation 6 does not consider the dependence of the Sherwood number on the Schmidt number (Equation 5) because of the limited range of aqueous phase viscosities and organic diffusivities employed in this study. Other researchers have reported that the Sherwood number is proportional to the Schmidt number to a power between 0.33 and 0.67 (*27*,*32*-*35*). Figure 4 demonstrates the utility of the above correlation, for the prediction of initial dissolution behavior of styrene entrapped in the two sandy soils. Here, an interphase mass transfer expression of the form given in Equation 2 was incorporated into an aqueous phase transport equation and solved for steady-state effluent concentrations at a number of flow velocities. Observe that the experimental and predicted concentrations for the two sands at the various flow rates agree quite well.

In a similar systematic investigation of the initial volatilization of entrapped NAPLs in the same sandy media, Wilkins et al. (*4*) developed a correlation for the organic-gas lumped mass transfer coefficient. This correlation was expressed in terms of the Peclet number, an alternative dimensionless number containing velocity. The following correlation expression is based upon a reanalysis of their data in terms of Reynolds number:

$$Sh^{og} = 10^{-2.62} Re^{0.62} \delta^{1.82} \qquad [7]$$

Here Reynolds and Sherwood numbers are expressed in terms of gas phase properties. Similar to Equation 6, a multiple linear regression technique was used to determine the best fit correlation for the experimental data. The coefficient of multiple determination and standard error estimate for Equation 7 were found to be 0.99 and 0.067, respectively. The correlation was developed for a range of Reynolds numbers (0.04-1.2), and mean grain sizes (0.024-0.12 cm). The dependence of the Sherwood number on the Schmidt number (Equation 5) was again not considered in the development of Equation 7 because of the limited range in experimental gaseous phase viscosities and organic diffusivities employed in this study.

To directly compare these two correlations and to help develop further insight into the mass transfer process, it is useful to recast Equations 6 and 7 into an explicit expression for the lumped mass transfer coefficient. Thus, the dissolution and volatilization lumped mass transfer coefficients were found to be proportional to the following parameters:

$$\hat{k}^{ow} \propto v_w^{0.6} d_{50}^{-0.73} U^{0.37} \qquad [8]$$

$$\hat{k}^{og} \propto v_g^{0.62} d_{50}^{0.44} \qquad [9]$$

In comparing these two expressions, the first point to note is that the flow rate dependence of volatilization is strikingly similar to that of dissolution. In Equations 6 and 7 the Sherwood numbers also exhibit a similar dependence on Reynolds number. This suggests that the flowing phase fluid dynamics (water or gas) are similar in the two- and three-phase systems for the range of Reynolds numbers considered herein; i.e., $0.04<Re<0.20$. In contrast, however, exponents associated with porous media properties are quite dissimilar. For dissolution, the mass transfer coefficient is inversely proportional to the mean grain size, whereas for volatilization, the mass transfer coefficient is directly proportional to d_{50}. In addition, no statistically significant dependence on medium uniformity was observed for volatilization mass transfer. These differences in parameter dependency can be explained in terms of the conceptual models presented in Figure 1. In the three-phase systems, the mobile phase (gas) occupies the largest pores. As the mean grain size is reduced, increased capillary forces will tend to increase the residual water saturation, restricting gas flow and potentially further limiting gas access to the regions of entrapped NAPL. In contrast for NAPL dissolution, the flowing phase is water, the wetting fluid. Thus, a reduction in grain size will not limit pore accessibility to water. It will, however, influence the entrapped NAPL configuration, decreasing the mean size of entrapped ganglia and

increasing specific interfacial area and, hence, mass transfer. The data suggest that NAPL entrapment geometry in the three-phase system is comparatively unaffected by changes in grain size distribution.

The experimental correlations presented above were developed to represent the initial (quasi-steady) interphase mass transfer of organic compounds from entrapped NAPLs in saturated and unsaturated porous media. These correlations are appropriate for the estimation of the initial concentrations in soil water and gas phases following a contamination event. Exploration of the long-term persistence of entrapped NAPL residuals in such environments, however, requires the examination of mass transfer behavior over larger time scales. In this case, the lumped mass transfer coefficient may vary temporally due to changes in the interfacial area with deceasing NAPL saturation.

Figure 5 presents effluent concentration data from a single prolonged styrene dissolution experiment in Ottawa (quartz) sand. In this experiment, superficial velocity was held constant at 9.13 m/day. The figure plots the log of normalized concentration versus the number of pore volumes of water displaced. For simplicity, one pore volume is defined here such that it is equivalent to the total volume of voids in the column. Examination of the figure reveals that effluent concentrations are initially within 65% of the equilibrium solubility. As the styrene dissolves, however, concentrations begin to fall smoothly. Because the flow velocity is constant, this reduction in concentration implies a significant reduction in the lumped mass transfer coefficient with the removal of NAPL mass. Recall that the lumped mass transfer coefficient is a product of a mass transfer coefficient, presumed to be a function of system hydrodynamics and flowing fluid properties, and a specific interfacial area. Consider again the conceptual model presented in Figure 1A. Here NAPL is entrapped as isolated globules or interconnected ganglia. As NAPL mass dissolves, the ganglia will decrease in size. This decrease in size will be accompanied by a corresponding decrease in exposed interfacial area. It is likely that the larger ganglia, which have smaller area-to-volume ratios, will tend to persist. Due to the reduction in interfacial area, concentrations will tend to decrease with dissolution. This hypothesis has been supported by measurements of ganglia (*in situ* polymerized styrene) size distributions in porous media and their correlation with mass transfer rates (*12*,*41*). Powers et al. (*41*) found that a decreasing d_{50} was associated with a decrease in the mean entrapped ganglia size and an increase in the mass transfer coefficient, whereas an increasing *U* was associated with an increase in the ganglia size distribution uniformity index and a higher initial mass transfer coefficient.

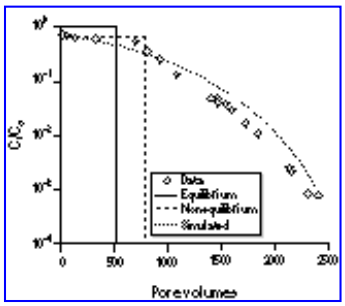

Figure 5. A plot of the log of the observed and predicted normalized styrene effluent concentration data versus pore volumes of water displaced through Ottawa sand at a superficial velocity 9.13 m/day (*41*); the porosity was 0.368 and the initial organic saturation was 0.132.

Surrogate parameters for interfacial area can be incorporated in correlations for mass transfer behavior to facilitate the prediction of the long-term persistence of NAPLs in the subsurface (*12*,*27*,*28*,*41*). To date, changes in interfacial area have been modeled with a power function of the NAPL saturation (*12*,*27*,*28*), or by assuming that the residual NAPL is entrapped as several sizes of spherical globules with known radii (*41*). Figure 5 illustrates predictions for the long-term dissolution behavior of styrene based upon a number of modeling approaches: *a*) assumption of a constant equilibrium effluent concentration; *b*) assumption of a constant (nonequilibrium) concentration determined from the lumped mass transfer correlation (Equation 6) and use of a steady-state analytic solution for solute transport that neglects dispersion; and *c*) use of a numerical solute transport simulator that incorporates the linear driving force model (Equation 2) and the lumped mass correlation (Equation 6) modified with a power function of the relative organic saturation (12) as a surrogate of interfacial area. Note that many of the organic chemicals commonly entrapped as NAPLs in the subsurface have regulated concentration levels in the part or tens of parts per billion range, while solubilities are several orders of magnitude greater. Reduction to such concentration levels is predicted for cases *a*, *b*, and *c* after 525, 805, and 2440 pore volumes, respectively. The experimental data shown in Figure 5 indicate that approximately 2420 pore volumes are required to completely dissolve the entrapped styrene. Here the numerical modeling approach based upon Equations 2 and 6 was the best predictor of this remediation time, whereas both the steady nonequilibrium and equilibrium approaches greatly under estimated this time. Note that the percentage of the total styrene mass recovered from the experimental system at 525, 805, and 2440 pore volumes equals 82, 86, and 100%, respectively. This observation suggests that remediation efficiency decreases with decreasing organic mass because of mass transfer limitations caused by temporal changes in the organic-water interfacial area.

An example data set from an entrapped styrene volatilization experiment in the same sand is shown in Figure 6. Here again, concentration levels fall as NAPL removal proceeds. In contrast to the dissolution case, however, effluent concentrations (and consequently mass transfer rates) remain high over most of the experiment. The sharp drop in effluent concentration coincides with removal of more than 99% of the NAPL mass within the column. A similar rapid decline in concentration has been observed in other volatilization studies (*38*,*42*). These observations suggest that the specific interfacial area remained relatively constant during the volatilization experiment. This hypothesis is consistent with the conceptual model of entrapped NAPL configuration as thin films (Figure 1B). Further examination of Figure 6 reveals that the sharp concentration decrease is followed by an extended period of low but persistent concentration levels. This concentration tail may be caused by the presence of small zones of occluded NAPL or by rate limitations in desorption of styrene from the soil.

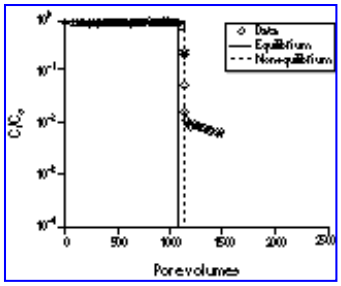

Figure 6. A plot of the log of the observed and predicted (Equation 7) normalized styrene effluent concentration data versus pore volumes of air displaced through Ottawa sand at a superficial velocity of 30.24 m/day (*15*); the porosity was 0.35, the initial organic saturation was 0.048, and the residual water saturation was 0.071.

Figure 6 also presents predictions for the long-term volatilization behavior of styrene based upon *a*) assumption of a constant equilibrium effluent concentration; and *b*) assumption of a constant (nonequilibrium) concentration determined from the lumped mass transfer correlation (Equation 7) coupled with a steady-state analytic solution for solute transport that neglects dispersion (*4*). In contrast to the dissolution behavior shown in Figure 5, Figure 6 suggests that temporal changes in the lumped mass transfer coefficient need not be modeled to predict long-term volatilization behavior, because of the presence of uniform effluent concentration levels over most of the period of styrene removal. Complete styrene recovery is predicted for cases *a* and *b* after 1091 and 1146 pore volumes, respectively. The experimental data indicate that approximately 1180 pore volumes are required to recover 99.8% of the entrapped styrene. The approach that assumed constant nonequilibrium concentrations was the best predictor of this remediation time. The equilibrium assumption provides a better prediction of volatilization than dissolution behavior, but still underestimates the remediation time compared to case (*b*). The percentage of the total styrene mass recovered from the experimental system at 1091 and 1146 pore volumes equals 98.3 and 99.4%, respectively. These observations suggest that volatilization predictions should consider rate-limited mass transfer, but that temporal changes in interfacial area do not have to be explicitly modeled. For further discussion of these issues, the interested reader is referred to Abriola et al. (*15*).

Nonaqueous-Phase Liquid Mixtures

The preceding section presented data related to the dissolution and volatilization of pure (single chemical component) organic liquid contaminants. NAPLs found at contaminated waste sites, however, are commonly composed of mixtures of several organic species (*43*). Examples of NAPL mixtures include transformer oil containing polychlorinated biphenyls (*44-45*), coal tars and creosotes (*46*), gasoline (*47*), diesel fuel (*48*), petroleum products (*49*), and various chlorinated solvents used in industrial operations (*50*). The interaction of components in NAPL mixtures may create substantial differences in the mass transfer characteristics of a given component in comparison with the behavior of the pure compound (*51*). Hence, an accurate description of the partitioning behavior of complex NAPLs is essential to the prediction and assessment of contamination concentrations in the environment.

When dealing with NAPL mixtures, it is useful to recast the linear driving force expression given in Equation 2 in terms of mole fraction, x_{ai} (moles *i*/moles solution):

$$E_i^{\alpha} = \rho_{\alpha}^{m} M_i \hat{k}_i^{\circ\alpha} \left(x_{\alpha i}^{eq} - x_{\alpha i} \right) \qquad [10]$$

Here $x_{\alpha i}^{eq}$ is the equilibrium mole fraction of the organic component *i* in the α phase, ρ_{α}^{m} is the molar density (moles L^{-3}) of the α phase, and M_i is the molecular weight of component *i.* Note that the bulk α phase

concentration of organic component *i* ($C_{\alpha,i}$) is equal to $\rho_{\alpha}^{m} M_i x_{\alpha,i}$. The equilibrium mole fraction of the organic component in the α phase can be related to the mole fraction of this same species in the organic phase (x_{oi}) according to the following equation (*52*):

$$x_{\alpha i}^{eq} = x_{\alpha i}^{*eq}\left(\frac{\gamma_{oi} f_{oi}}{f_{oi}^{*}}\right) x_{oi} = K_i^{\alpha\alpha} x_{oi} \qquad [11]$$

Here γ_{oi} and f_{oi} are the activity coefficient and reference state fugacity, respectively, of component *i* in the organic phase, f_{oi}^{*} is the reference state fugacity of the pure organic compound, $x_{\alpha i}^{*eq}$ is the equilibrium mole fraction of the pure organic compound in the α phase, and $K_i^{\alpha\alpha}$ is known as the equilibrium partition coefficient. Equation 11 is based on the principle that the chemical potentials in each phase are equal at thermodynamic equilibrium (*53*) and assumes that the activity coefficient of component *i* in the α phase is independent of x_{oi}.

The direct determination of equilibrium partition coefficients for all relevant organic components into the water and air phases can be time-consuming, experimentally difficult, and expensive. If ideal behavior of the organic phase is assumed in Equation 11 (i.e., organic activity coefficient of unity and identical reference state fugacities), estimates of $K_i^{\alpha\alpha} = x_{\alpha i}^{*eq}$ can be obtained directly from solubility (*54*) or vapor pressure data (*55*) for the pure organic compound according to a generalized form of Raoult's Law (*50*):

$$x_{\alpha i}^{eq} = x_{\alpha i}^{*eq} x_{oi} \qquad [12]$$

The assumption of ideal organic behavior is reasonable for NAPL mixtures composed of chemically similar components (*56*,*57*). Note that Equations 11 and 12 can be recast in terms of concentrations by multiplying by $\rho_{\alpha}^{m} M_i$ or in terms of vapor pressures by invoking the Ideal Gas Law.

Based upon the linear driving force expression (Equation 10), Raoult's Law (Equation 12), and the modified Sherwood correlation (Equation 7), predictions may be obtained for volatilization of an organic liquid mixture entrapped in sandy soils. To explore the accuracy of this predictive approach, a systematic laboratory investigation was undertaken to extend the observations of Wilkins et al. (*4*) to two-component organic mixtures. Preliminary results of this investigation were presented in Gaither and Abriola (*13*). A complete description of the research work will be forthcoming. Data from some of the experiments are presented in Figures 7 and 8 to highlight the important laboratory findings.

A series of volatilization experiments was conducted for a binary mixture of styrene and toluene in one sandy medium. Wagner sand was employed in this study as well as in earlier dissolution (*6*,*12*) and volatilization (*4*) experiments. Here, three distinct binary (mole fraction) mixtures, 0.5 toluene/0.5 styrene, 0.8 toluene/0.2 styrene, and 0.2 toluene/0.8 styrene, were used. Effluent gas concentrations were measured over a range of flow rates (40-400 ml/min) to simulate conditions typically encountered during field soil vapor extraction operations (*58*). Mass transfer coefficients were estimated from these data using the linear driving force expression (Equation 10) in conjunction with Raoult's Law (Equation 12), and the saturated vapor concentrations of pure styrene and toluene (40.1 and 140.5 mg/l, respectively). Figure 7 presents a comparison of the experimentally determined Sherwood numbers with those predicted using Equation 7. Note that measured and predicted values of the Sherwood number agree reasonably well, as indicated by a coefficient of linear regression equal to 0.898. A slight deviation from the predicted Sherwood number is observed for the lower mole fraction organic components, i.e., the observed effluent concentration was lower than that predicted using Raoult's Law and the correlation developed for pure NAPLs. This result may be due to additional diffusional limitations within a NAPL boundary layer that are not incorporated in the linear driving force model, or some nonideality of the NAPL mixture, creating deviations from equilibrium vapor pressure predictions using Raoult's Law.

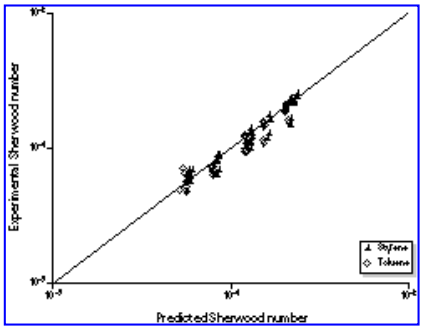

Figure 7. A plot of the experimentally determined Sherwood numbers for binary NAPL mixtures composed of toluene and styrene vs the predicted Sherwood numbers determined for pure NAPLs (Equation 7) (*13*).

Recall that the correlation presented in Figure 7 was developed for the prediction of initial volatilization rates. To investigate the long-term volatilization behavior for the various NAPL mixtures, additional column experiments were conducted. In these experiments, flow rates were maintained at low levels to achieve close to equilibrium conditions at the initiation of volatilization. Figure 8 shows results of one experiment. Here the log of normalized effluent concentration is plotted versus pore volumes of gas for the NAPL mixture composed of 0.8 toluene and 0.2 styrene (mole fractions). Note that concentrations are normalized with respect to the saturated gas phase concentration of the pure organic liquid. Examination of the figure reveals that the relative concentrations for both toluene and styrene are initially determined by their mole fractions in the binary mixture, as predicted by Raoult's law. As in the pure NAPL volatilization experiments (Figure 6), these relative concentrations are maintained over many pore volumes, presumably due to the pore scale distribution of interfacial area as continuous films (Figure 1B). As one component becomes depleted, however, the behavior differs from the pure NAPL case. A rapid drop in the effluent concentration of the more volatile component (toluene) is accompanied by an increase in the mole fraction of the remaining constituent (styrene) to near-saturated values. Again, these observations are consistent with ideal partitioning behavior as predicted by Raoult's Law. Note that here an increase in styrene concentration actually reflects NAPL mass reduction. This experiment illustrates that large variations in component concentration can be caused by changing NAPL composition. Similar behavior has been observed in column vapor extraction investigations using more complex NAPL mixtures (*38*,*39*). Figure 8 reveals that eventually the majority of the remaining NAPL component mass is removed. This removal is accompanied by a dramatic decrease in the air-NAPL interfacial area, followed by a sharp decline in the effluent concentration. As discussed above, the observed concentration tailing behavior for both components is likely due to rate-limited desorption, and/or the presence of less accessible residual organic. These experimental observations suggest that the volatilization, disappearance rate, and associated gas phase concentrations for binary organic liquid mixtures under natural or remediation conditions can be adequately predicted with the linear driving force expression, coupled with Raoult's Law (Equation 12) and a correlation (Equation 7) representative of initial volatilization rates.

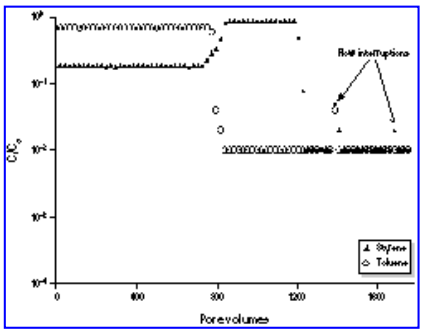

Figure 8. A plot of the log of normalized effluent concentrations (with respect to the saturated gas phase concentration of the pure organic) vs pore volumes of gas for the binary NAPL mixture (composed of 0.8 toluene and 0.2 styrene) entrapped in the Wagner sand (*13*). The superficial velocity was 30.24 m/day and the initial organic saturation was 0.111.

The assumption of organic liquid phase ideality has also been used successfully by a number of investigators to describe the equilibrium dissolution of polynuclear aromatic hydrocarbons (PAHs) from DNAPLs such as creosotes and coal tars (*48*,*59-61*). Significant deviations from ideality, however, have been reported in some cases (*48*). Furthermore, rigorous validation of the use of Raoult's law has been compounded by difficulty in completely characterizing field coal tar samples. To more conclusively address this issue, a laboratory batch

study was undertaken to investigate the dissolution behavior of a number of synthetic, compositionally well-defined, coal tar mixtures (*16*). Mixtures were composed of toluene and eight PAHs: naphthalene, 1-methylnapthalene, 2-ethylnaphthalene, acenaphthene, fluorene, phenanthrene, fluoranthene, and pyrene. Experiments were conducted in a custom-designed mixed reactor system, consisting of a cylindrical reservoir that had been fused to the bottom of a 1000-ml three-necked flask. The design of the reactor was such that a constant DNAPL-water interfacial area was maintained throughout the course of the experiment at the juncture between the cylindrical reservoir and the flask. Both fluids were mixed continuously and the aqueous phase was sampled periodically until equilibrium between the phases was achieved (over 5-7 days). Further details pertaining to the experimental protocol and preparation of the synthetic DNAPL mixtures may be found in Mukherji et al. (*16*).

The multicomponent dissolution process occurring in the reactor was subsequently modeled with a linear driving force expression (Equation 10) and the equilibrium partitioning relation (Equation 11). Values of the mass transfer and equilibrium partition coefficients for the various DNAPL components were determined by fitting this model to the observed time-dependent aqueous phase concentrations. The fitted mass transfer coefficients for this water-DNAPL batch system will not be discussed further herein. The interested reader is referred to Mukherji et al. (*16*) for a complete presentation of these coefficients.

The fitted equilibrium partition coefficients were used to assess the assumption of organic phase ideality (γ_{oi}=1) to predict equilibrium aqueous phase concentrations. Here, an estimate of the ratio of the reference state fugacities is required, as some of the NAPL components are solids in their pure form at room temperature. Two methods to determine this ratio (f_{oi}/f^{*}_{oi}) were explored: method 1 based on an assumption of a constant energy of fusion (*62*); and method 2, a more general thermodynamic approach (*53*). Table 2 presents calculated values of f_{oi}/f^{*}_{oi} for the various DNAPL components of one synthetic coal tar mixture based upon each method. Values of γ_{oi} that were subsequently calculated from Equation 11 are also given in the table. Note in Table 2 that values of f_{oi}/f^{*}_{oi} calculated according to method 2 lead to predictions of γ_{oi} that are consistently closer to unity than those based on method 1. This result suggests that values of f_{oi}/f^{*}_{oi} calculated according to method 2 are more reasonable, and that the assumption of organic phase ideality (γ_{oi}=1) is reasonably good for this model DNAPL mixture. This conclusion was also supported by equilibrium measurements with other synthetic DNAPL mixtures.

Table 2. Calculated values of γ_{oi} and f_{oi}/f^{*}_{oi} for organic components of the synthetic DNAPL mixture (*16*) according to method 1 (*62*) and method 2 (*53*).

Compound	Method 1		Method 2	
	γ_{oi}	f_{oi}/f^{*}_{oi}	γ_{oi}	f_{oi}/f^{*}_{oi}
Toluene	1.250	1.000	1.250	1.000
Naphthalene	0.920	3.534	1.000	3.268
1-Methylnaphthalene	1.060	1.000	1.060	1.000
2-Ethylnaphthalene	1.050	1.000	1.050	1.000
Acenaphthene	0.780	5.051	0.790	4.975
Fluorene	0.720	7.937	0.910	6.250
Phenanthrene	0.640	5.650	1.000	3.584
Fluoranthene	0.560	7.092	0.850	4.695
Pyrene	0.350	19.61	0.750	9.346

Fractional Wettability Soils

The foregoing discussion and experiments focused on the entrapment and mass transfer behavior of NAPLs in water-wet porous media. This has also been true of most previous experimental dissolution studies, which were conducted in water-wet glass beads or silica sands where the residual NAPL was entrapped primarily as singlets or multipore ganglia (Figure 1A) (*6*,*27*-*31*). Natural subsurface systems, however, may exhibit pronounced variations in solid surface properties. For example, spatial and/or temporal changes in aqueous chemistry (*63*), mineralogy (*64*), organic matter distributions (*65*), surface roughness (*66*), and contaminant aging (*67*) can give rise to variations in wetting properties. When both water- and organic-wet sites are present in a medium, this condition is referred to as fractional wettability. In the petroleum literature, fractional wettability has been recognized as a ubiquitous condition (*68*-*70*). An understanding of the influence of wettability variations on the pore-scale configuration of residual NAPL and the subsequent interphase mass transfer will thus be required to assess the persistence of NAPLs in natural soils.

Figure 9 presents a conceptual model of residual NAPL distribution in a two-liquid-phase fractional wettability system. Note that the residual NAPL includes both multipore NAPL ganglia and singlets, as found in water-wet porous media (Figure 1A) as well as organic films coating some of the solid surfaces. It is anticipated that such changes in the pore-scale distribution of residual NAPL will lead to differences in the organic-water interfacial area (*71*) and the aqueous flow field (*72*). For a soil at a given NAPL saturation, the organic-water interfacial area will be much higher when the NAPL is distributed as a film than when it is entrapped as a singlet or ganglia (*73*).

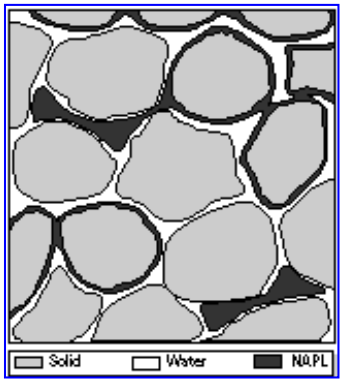

Figure 9. Hypothetical distribution of residual NAPL in the saturated zone when the porous medium has fractional wettability.

To explore the influence of fractional wettability on the entrapment and dissolution of a residual NAPL, tetrachloroethylene (PCE), a series of experiments was conducted with synthetic soils (*14*). The porous medium employed in these experiments was a mixture of two sieve sizes of Ottawa sands. Some of these sands were treated with a 2 to 3% solution of octadecyltrichlorosilane (OTS) in ethanol to render them organic-wet (*74*). Fractional wettability media were then obtained by mixing untreated and OTS-treated Ottawa sands to obtain 0, 25, 50, 75, and 100% by weight OTS media. Custom-designed aluminum columns, 4.8 cm long and 5 cm inside diameter, were subsequently packed with the various fractional wettability media. Residual PCE entrapment was achieved in a similar manner to that previously discussed for the water-wet media. Further details of the experimental methodology are provided in Bradford et al. (*14*).

After PCE entrapment, columns were flushed with Milli-Q water to explore dissolution mass transfer in these fractional wettability systems. Figure 10 presents a plot of the log of normalized effluent concentrations (with respect to the equilibrium concentration) versus pore volumes of water flowing through the columns. Effluent concentration profiles for different fractional wettability porous media are shown. In general, measured effluent concentrations were initially near equilibrium, then decreased over time and exhibited extended tailing. Note, however, that differences in the media's wettability dramatically affected the dissolution behavior. For a given residual PCE saturation, an increasing organic-wet fraction resulted in longer periods of high effluent concentrations, followed by a more rapid decrease of the concentration, and finally lower concentrations in the tailing region. Note also that the dissolution behavior for the 100% OTS sand is similar to the volatilization behavior observed for a three-phase water-wet medium (Figure 6). This observation can be attributed to the comparable pore-scale configuration of the residual organic in both systems.

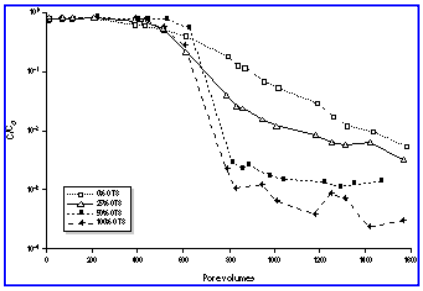

Figure 10. A log plot of the normalized effluent concentrations versus pore volumes of water for PCE entrapped in Ottawa sand composed of 0, 25, 50, and 100% OTS mass fractions (*14*). The initial organic saturation for the 0, 25, 50, and 100% OTS sands were 0.065, 0.060, 0.069, and 0.059, respectively; the corresponding superficial velocities were 6.58, 6.58, 6.79, and 6.56 m/day, respectively.

A possible explanation for the dissolution behavior shown in Figure 10 is suggested by considering the conceptual model of PCE distribution in fractional wettability media (Figure 9). In fractional wettability media it is likely that the residual PCE is entrapped both as films covering organic-wet solids and as larger ganglia near water-wet solids. The relative proportion of PCE entrapped as films and ganglia depends largely on the fractional wettability. The area per volume ratio of the entrapped NAPL would be much higher when the PCE is distributed as films than when it occurs as ganglia (*73*). Consequently, the presence of PCE films is likely responsible for the longer periods of high effluent concentrations. Once the PCE films are dissolved, a dramatic decrease in interfacial area is hypothesized to occur, which would lead to a sudden dropoff in concentration. The tailing behavior is likely due to the presence of PCE ganglia that dissolve more slowly than the PCE films

because of their lower interfacial area per PCE volume ratio. The higher PCE concentrations in the tailing region with lower organic-wet fractions can be explained by assuming more of the entrapped PCE occurred as ganglia than as films in media with lower organic-wet fractions.

Summary and Implications

This paper has presented an overview of experimental research exploring NAPL entrapment and interphase mass transfer that has been conducted over the past several years at the University of Michigan. An understanding and quantification of these interphase mass transfer processes will be required to predict organic contaminant persistence in the subsurface, as well as the effectiveness of remedial technologies. In this work, a quasi-steady-state approximation of Fick's First Law, i.e., a linear driving force model, has served as the conceptual and mathematical framework for the description of rate-limited interphase mass transfer. In the context of this model, the key parameters controlling interphase mass transfer are the equilibrium partition coefficient, the mass transfer coefficient, and the interfacial area.

For pure NAPLs, equilibrium partitioning is relatively simple to characterize from solubility and vapor pressure data. In contrast, equilibrium mass transfer for multicomponent NAPLs is much more difficult to quantify. In such cases, additional information on the composition of the NAPL mixture, the solubility, the volatility, and the reference state fugacities of the individual constituents are required. Results from the studies presented herein suggests that the assumption of organic phase ideality is reasonable for many mixtures, if fugacities are determined appropriately. Results also indicate, however, that evaluating the equilibrium partitioning relations of complex NAPLs at hazardous waste sites will be a daunting task, especially when one considers the interactions of contaminant aging, biological transformations, and ill-defined initial NAPL characterization.

The mass transfer coefficient is a second fundamental parameter required to describe rate-limited interphase mass transfer. Lumped within this parameter are the effects of boundary layer diffusion, fluid velocity, viscosity, NAPL morphology, and pore structure. In the research reported herein, predictive correlations were developed relating experimentally determined lumped mass transfer coefficients (for constant interfacial areas) and relevant system parameters. Mass transfer coefficients for volatilization and dissolution showed similar dependencies on velocity, indicating comparable flowing phase fluid dynamics in these systems. When considering medium specific parameters, however, the volatilization mass transfer coefficient was found to be directly correlated to the mean soil grain size, whereas the dissolution mass transfer coefficient was inversely related to this parameter. This result, as well as sensitivity to porous medium uniformity, was explained by considering differences in entrapped NAPL morphology occurring in the saturated and unsaturated zones. Application of these correlations permits estimation of receptor concentrations and contamination persistence in a given scenario.

The research presented herein also demonstrates the importance of interfacial area in the determination of the initial and, most particularly, the long-term mass transfer of NAPLs. Prolonged mass transfer of NAPLs leads to changes in the NAPL saturation and, consequently, changes in the interfacial areas. When the residual NAPL was found primarily as films (organic-wet solids or spreading organic on an air-water interface), which have high interfacial areas, effluent concentrations were near equilibrium values until the vast majority of the NAPL mass was recovered. The subsequent drop in concentration, followed by concentration tailing at low levels, corresponds to a sudden decrease in the interfacial area. In contrast, residual NAPL configured as singlets and multipore ganglia, which have a relatively low interfacial area, produced gradually decreasing effluent concentrations as the ganglia slowly shrunk. Systems in which both films and ganglia occurred produced initially high effluent concentrations, followed by a sudden drop in concentration, and then more gradual changes in concentrations. These observations suggest that the long-term persistence of separate phase NAPL is controlled by the interfacial area; higher interfacial areas enhance NAPL remediation. Consequently, surrogate measures of interfacial area need to be incorporated into predictive models of interphase mass transfer.

The experimental studies presented herein have identified key parameters that must be considered in investigations of interphase mass transfer. Significant research efforts at the University of Michigan have also been made to incorporate this information into numerical multiphase flow and transport simulators (*6,15,23,41,75,76*). Numerical experiments have subsequently been undertaken to investigate the implications of rate-limited mass transfer at a variety of scales (column to field), and to explore complex interactions between interphase volatilization, dissolution, sorption, and biological transformations. The insight gained from these numerical studies has synergistically stimulated new experimental endeavors. Ongoing research sponsored by the NIEHS is currently directed towards the incorporation of interfacial area estimates into correlations of interphase mass transfer, the quantification of rate limitations in concentration tailing regions, and the interaction of interphase mass transfer and bioavailability.

Appendix: Notation

α water (w) or gas (g) phase

γ_{oi} activity coefficient of component *i* in organic phase

δ dimensionless mean grain size equal to d_{50}/d_M

μ_α viscosity of the α phase ($ML^{-2}T^{-1}$)

ρ_α density of the α phase (ML^{-3})

ρ_α^m molar density of the α phase (mole L^{-3})

$a^{o\alpha}$ organic and α phase interfacial area per unit volume of porous media (L^{-1})

C_α bulk phase concentration of the organic in the α phase (ML^{-3})

C_α^{eq} equilibrium concentration of the organic in the α phase (ML^{-3})

D_α diffusivity of the organic in the α phase (L^2T^{-1})

d_{10} diameter of soil grain where 10% of the soils grains are smaller (L)

d_{50} diameter of soil grain where 50% of the soils grains are smaller (L)

d_{60} diameter of soil grain where 60% of the soils grains are smaller (L)

d_M mean grain size of a medium sand equal to 0.05 cm (L)

$E_i^{o\alpha}$ total mass flux per unit volume between the component *i* and the α phase ($ML^{-3}T^{-1}$)

$E^{o\alpha}$ total mass flux per unit volume between the organic and α phases ($ML^{-3}T^{-1}$)

f_{oi} reference state fugacity of component *i* in the organic phase

f_{oi}^* reference state fugacity of the pure organic compound

g denotes gas phase

i denotes organic component

$J^{o\alpha}$ flux of the organic to the α phase ($ML^{-2}T^{-1}$)

$K_i^{o\alpha}$ equilibrium partition coefficient

$k^{o\alpha}$ **mass transfer coefficient (LT^{-1})**

$\hat{k}^{oa}$ **lumped mass transfer coefficient (T^{-1})**

M_i **molecular weight of component *i* ($M\ mole^{-1}$)**

o **denotes organic phase**

R **multiple correlation coefficient**

Re **Reynolds number (Equation 4)**

Sc **Schmidt number (Equation 5)**

$Sh^{o\alpha}$ **Sherwood number for mass transfer between the organic and α phase (Equation 3)**

U **uniformity index equal to d_{60}/d_{10}**

v_α **average pore velocity of the α phase (LT^{-1})**

w **denotes water phase**

$x^{*eq}_{\alpha i}$ **equilibrium mole fraction of pure organic component *i* in the α phase**

$x^{eq}_{\alpha i}$ **equilibrium mole fraction of organic component *i* in the α phase**

$x_{\alpha i}$ **mole fraction of organic component *i* in the α phase**

x_{oi} **mole fraction of organic component *i* in the organic phase**

References and Notes

1. National Research Council. Alternatives for Ground Water Cleanup. Washington:National Academy Press, 1994.

2. Dragun J, Kuffner AC, Schneiter RW. Groundwater contamination. Part I: Transport and transformations of organic chemicals. Chem Eng 91:65-70 (1984).

3. Kavanaugh MC, Contaminant site remediation--technology versus public-policy. Water Environ Res 68:963-964 (1996).

4. Wilkins MD, Abriola LM, Pennell KD. An experimental investigation of rate-limited NAPL volatilization in unsaturated porous media: steady-state mass transfer. Water Resour Res 31:2159-2172 (1995).

5. Mayer AS, Miller CT. The influences of porous medium characteristics and measurement scale on pore-scale distributions of residual nonaqueous phase liquids. J Contam Hydrol 11:189-213 (1992).

6. Powers SE, Abriola LM, Weber WJ Jr. An experimental investigation of NAPL dissolution in saturated subsurface systems: steady-state mass transfer rates. Water Resour Res 28:2691-2705 (1992).

7. Rathfelder KM, Lang JR, Abriola LM. Soil vapor extraction and bioventing: applications, limitations, and future research directions. Rev Geophys IUGG Quadrenn Report 33:1067-1081 (1995).

8. Pennell KD, Abriola LM, Weber WJ Jr. Surfactant-enhanced solubilization of residual dodecane in soil columns. 1: Experimental investigations. Environ Sci Technol 27:2332-2340 (1993).

9. Abriola LM, Dekker TJ, Pennell KD. Surfactant-enhanced solubilization of residual dodecane in soil columns. 2: Mathematical modelling. Environ Sci Technol 27:2341-2351 (1993).

10. Burris DR, Antworth CP. *In situ* modification of an aquifer material by a cationic surfactant to enhance retardation of organic contaminants. J Contam Hydrol 10:325-337 (1992).

11. Xu S, Boyd SA. Cationic surfactant sorption to a vermiculitic subsoil via hydrophobic bonding. Environ Sci Technol 29:312-320 (1995).

12. Powers SE, Abriola LM, Weber WJ Jr. An experimental investigation of NAPL dissolution in saturated subsurface systems: transient mass transfer rates. Water Resour Res 30:321-332 (1994a).

13. Gaither CL, Abriola LM. An experimental investigation of the volatilization of binary NAPL mixtures in unsaturated porous media. In: Joint Conference on the Environment Abstracts Book, Hazardous Substance Research Center (HSRC)/Waste-management Education & Research Consortium (WERC), Albuquerque, New Mexico, 21-23 May, 1996;70-71.

14. Bradford SA, Abriola LM, Vendlinski RA. Entrapment and dissolution of tetrachloroethylene in fractional wettability porous media. EOS 77:F274 (1996).

15. Abriola LM, Pennell KD, Weber WJ Jr, Lang JR, Wilkins MD. Persistence and interphase mass transfer of organic contaminants in the unsaturated zone: experimental observations and mathematical modeling. In: Vadose Zone Hydrology: Cutting Across Disciplines (Parlange JY, Hopmans JW, eds). New York:Oxford University Press, in press.

16. Mukherji S, Peters CA, Weber WJ Jr. Mass transfer of polynuclear aromatic hydrocarbons from complex DNAPL mixtures. Environ Sci Technol 31:416-423 (1997).

17. Anderson WG. Wettability literature survey. Part 4: Effects of wettability on capillary pressure. J Petro Technol 39:1283-1299 (1987).

18. Wilson JL, Conrad SH, Mason WR, Peplinski W, Hagan E. Laboratory investigation of residual liquid organics from spills, leaks and the disposal of hazardous wastes in groundwater. EPA/600/6-90/004 (1990).

19. Blunt MJ, Fenwick DH, Zhou D. Unpublished data.

20. Hayden NJ, Voice TC. Microscopic observations of a NAPL in a three-fluid-phase soil system. J Contam Hydrol 12:217-226 (1993).

21. Weber WJ Jr, McGinley PM, Katz LE. Sorption phenomena in subsurface systems: concepts, models and effects on contaminant fate and transport. Water Res 25:499-528 (1991).

22. de Zabala EF, Radke CJ. A non-equilibrium description of alkaline water flooding. SPE Reservoir Eng 2:29-43 (1986).

23. Powers S, Loureiro CO, Abriola LM, Weber WJ Jr. Theoretical study of the significance of nonequilibrium dissolution of nonaqueous phase liquids in subsurface systems. Water Resour Res 27:463-477 (1991).

24. Borden RC, Kao C-M. Evaluation of groundwater extraction for remediation of petroleum-contaminated aquifers. Water Environ Res 64:28-36 (1992).

25. Brusseau ML. Rate-limited mass transfer and transport of organic solutes in porous media that contain immobile immiscible organic liquid. Water Resour Res 28:33-46 (1992).

26. Hatfield K, Stauffer TB. Transport in porous media containing residual hydrocarbon. 1: Model. J Environ Engr 119:540-558 (1993).

27. Miller CT, Poirier-McNeill MM, Mayer AS. Dissolution of trapped nonaqueous phase liquids: mass transfer characteristics. Water Resour Res 26:2783-2796 (1990).

28. Imhoff PT, Jaffe PR, Pinder GF. An experimental study of complete dissolution of a nonaqueous phase liquid in a saturated porous media. Water Resour Res 30:307-320 (1993).

29. Pfannkuch HO. Ground-water contamination by crude oil at the Bemidji, Minnesota, research site: US Geological Survey Toxic Waste--Ground-Water Contamination Study. Water-Resources Investigations Rpt 84-4188. Reston, VA:US Geological Survey, 1984.

30. Parker JC, Katyal AK, Kaluarachchi JJ, Lenhard RJ, Johnson TJ, Jayaraman K, Unlu K, Zhu JL. Modeling multiphase organic chemical transport in soils and ground water. EPA/600/2-91/042. Washington:U.S. Environmental Protection Agency, 1991.

31. Guarnaccia JF, Imhoff PT, Missildine BC, Oostrom M, Celia MA, Dane JH, Jaffe PR, Pinder GF. Multiphase chemical transport in porous media. EPA/600/S-92/002. Washington: U.S. Environmental Protection Agency, 1992.

32. Imhoff PT, Frizzell A, Miller CT. Evaluation of thermal effects on the dissolution of a nonaqueous phase liquid in porous media. Environ Sci Technol 31:1615-1622 (1997).

33. Dwivedi PN, Updhyay SN. Particle-fluid mass transfer in fixed and fluidized beds. Ind Eng Chem, Process Design Develop 16:157-165 (1977).

34. Kumar S, Updhyay SN, Mathur VK. Low Reynolds number mass transfer in packed beds of cylindrical particles. Ind Eng Chem, Process Design Develop 16:1-8 (1977).

35. Williamson JE, Bazazaire KE, Geankoplis CJ. Liquid-phase mass transfer at low Reynolds numbers. Ind Eng Chem Fund 2:126-129 (1963).

36. Hunt JR, Sitar N, Udell KS. Nonaqueous phase liquid transport and cleanup. 1: Analysis of mechanisms. Water Resour Res 24:1247-1258 (1988).

37. Baehr AL, Hoag GE, Marley MC. Removing volatile contaminants from the unsaturated zone by inducing advective air-phase transport. J Contam Hydrol 4:1-26 (1989).

38. Bloes MB, Rathfelder KM, Mackay DM, Laboratory studies of vapor extraction for remediation of contaminated soil. In: Subsurface Contamination by Immiscible Fluids (Balkema AA, ed). Rotterdam/Brookfield, VT:AA Balkema, 1992;255-262.

39. Hayden NJ, Voice TC, Annable MD, Wallace RB. Change in gasoline constituent mass transfer during soil venting. J Environ Eng 120:1598-1614 (1994).

40. Driscoll FG. Groundwater and Wells. 2nd Ed. Minnesota:Johnson Filtration Systems, 1986.

41. Powers SE, Abriola LM, Dunkin JS, Weber WJ Jr. Phenomenological models for transient NAPL-water mass-transfer processes. J Contam Hydrol 16:1-33 (1994b).

42. Berndtson MJ, Bunge AL. A mechanistic study of forced aeration for in-place remediation of vadose zone soils. In: Proceedings of the Petroleum Hydrocarbons and Organic Chemicals in Ground Water:Prevention, Detection, and Restoration, Houston, TX. Dublin, OH:Waterwell Journal Publishing Co., 1991;249-263.

43. Powers SE, Villaume JF, Ripp JA. Multivariate analyses to improve understanding of NAPL pollutant sources. Ground Water Monitor Remed 17:130-140 (1997).

44. Roberts JR, Cherry JA, Schwartz FW. A case study of a chemical spill: polychlorinated biphenyls (PCBs). 1: History, distribution, and surface translocation. Water Resour Res 18:535-545 (1982).

45. Schwartz FW, Cherry JA, Roberts JR. A case study of a chemical spill: polychlorinated biphenyls (PCBs). 2: Hydrogeological conditions and contaminant migration. Water Resour Res 18:535-545 (1982).

46. Villaume JF. Coal tar wastes: their environmental fate and effects, hazardous and toxic wastes. In: Technology Management and Health Effects (Majumdar SK, Miller FW, eds). Easton, PA:Pennsylvania Academy of Sciences, 1984;362-375.

47. Cline PV, Delfino JJ, Rao PSC. Partitioning of aromatic constituents into water from gasoline and other complex solvent mixtures. Environ Sci Technol 25:914-920 (1991).

48. Lee LS, Rao PSC, Okuda I. Equilibrium partitioning of polycyclic aromatic hydrocarbons from coal tar into water. Environ Sci Technol 26:2110-2115 (1992).

49. Holzer TL. Application of groundwater flow theory to a subsurface oil spill. Ground Water 14:138-145 (1976).

50. Pankow JF, Cherry JA. Dense Chlorinated Solvents and Other DNAPLs in Groundwater. Guelph, ON, Canada:Waterloo Press, 1996.

51. Banerjee S. Solubility of organic mixtures in water. Environ Sci Technol 18:587-591 (1984).

52. Abriola LM. Modeling multiphase migration of organic chemicals in groundwater systems-a review and assessment. Environ Health Perspect 83:117-143 (1989).

53. Prausnitz JM. Molecular Thermodynamics of Fluid Phase Equilibria. Englewood Cliffs, NJ:Prentice Hall, 1969.

54. Mackay D, Shiu WY, Maijanen A, Feenstra S. Dissolution of non-aqueous phase liquids in groundwater. J Contam Hydrol 8:23-42 (1991).

55. Rathfelder KM, Yeh WW-G, Mackay D. Mathematical simulation of soil vapor extraction systems: model development and numerical examples. J Contam Hydrol 8:263-297 (1991).

56. Schwarzenbach RP, Gschwend PM, Imboden DM. Environmental Organic Chemistry. New York:John Wiley, 1993.

57. Adenekan AE, Patzek TW, Pruess K. Modeling of multiphase transport of multicomponent organic contaminants and heat in the subsurface: numerical model formulation. Water Resour Res 29:3737-3740 (1993).

58. Johnson PC, Stanley CC, Kemblowski MW, Byers DL, Colthart JD. A practical approach to the design, operation, and monitoring of *in-situ* soil venting systems. Ground Water Monitor Rev 10:159-178 (1990).

59. Picel KC, Stamoudis VC, Simmons M. Distribution coefficients for chemical components of a coal-oil/water system. Water Res 22:1189-1199 (1988).

60. Lane WL, Loehr RC. Estimating the equilibrium aqueous concentrations of polynuclear aromatic hydrocarbons in complex mixtures. Environ Sci Technol 26:983-990 (1992).

61. Luthy RG, Ramaswami A, Ghoshal S, Merkel W. Interfacial films in coal tar nonaqueous-phase liquid-water systems. Environ Sci Technol 27:2914-2918 (1993).

62. Mackay D, Shiu WY, Ma KC. Illustrated Handbook of Physical-Chemical Properties and Environmental Fate for Organic Chemicals. Vols 1, 2. Chelsea:Lewis Publishers, 1992.

63. Demond AH, Desai FN, Hayes KF. Effect of cationic surfactants on organic liquid-water capillary pressure-saturation relationships. Water Resour Res 30:333-342 (1994).

64. Anderson WG. Wettability literature survey. Part 1: Rock/oil/brine interactions and the effects of core

handling on wettability. J Petro Technol 38:1125-1144 (1986).

65. Dekker LW, Ritsema CJ. How water moves in a water repellent sandy soil. 1: Potential and actual water repellency. Water Resour Res 30:2507-2519 (1994).

66. Morrow NR. The effects of surface roughness on contact angle with special reference to petroleum recovery. J Can Petro Technol 14:42-53 (1975).

67. Powers SE, Tamblin ME. Wettability of porous media after exposure to synthetic gasolines. J Contam Hydrol 19:105-125 (1995).

68. Brown RJS, Fatt I. Measurements of fractional wettability of oilfield rocks by the nuclear magnetic relaxation method. Trans Am Inst Min Metall Pet Eng 207:262-264 (1956).

69. Donaldson EC, Thomas RD, Lorenz PB. Wettability determination and its effect on recovery efficiency. Soc Petro Eng J 9:13-20 (1969).

70. Salathiel RA. Oil recovery by surface film drainage in mixed-wettability rocks. J Petro Technol 255:1212-1224 (1973).

71. Bradford SA, Leij FJ. Estimating interfacial areas for multi-fluid soil systems. J Contam Hydrol 27:83-105 (1997).

72. Wang FHL. Effect of wettability alteration on water/oil relative permeability, dispersion, and flowable saturation in porous media. SPE Reservoir Engineering 4:617-628 (1988).

73. Gvirtzman H, Roberts PV. Pore scale spatial analysis of two immiscible fluids in porous media. Water Resour Res 27:1165-1176 (1991).

74. Anderson R, Larson G, Smith C. Silicon Compounds: Register and Review. 5th Ed. Piscataway, NJ:Huls America, 1991.

75. Lang JR, Rathfelder KM, Abriola LM. Multiphase, multicomponent numerical model of bioventing with nonequilibrium mass exchange. In: *In Situ* Aeration: Air Sparging, Bioventing, and Related Remediation Processes (Hinchee RE, Miller RN, Johnson PC, eds). Columbus, OH:Battelle Press, 1995;447-454.

76. Abriola LM, Lang J, Rathfelder KM. Documentation for: Michigan Soil-Vapor Extraction Remediation (MISER) Model --A Computer Program to Model Bioventing of Organic Chemicals in Unsaturated Geological Material. EPA/600/R97/0/99. Washington:U.S. Environmental Protection Agency, 1997.

Last Update: July 21, 1998